A contribution to exploring the importance of surface air nucleation in froth flotation – The effects of dissolved air on graphite flotation

Xu, M.; Li, C.; Zhang, H.; Kupka, N.; Peuker, U. A.; Rudolph, M.;

Originally published:

January 2022

Colloids and Surfaces A: Physicochemical and Engineering Aspects 633(2022), 127866

DOI: https://doi.org/10.1016/j.colsurfa.2021.127866

Perma-Link to Publication Repository of HZDR:

https://www.hzdr.de/publications/Publ-33855

A contribution to exploring the importance of surface air nucleation in froth flotation - the effects of dissolved air on graphite flotation

Ming Xu[a], Chenwei Li[b,c], Haijun Zhang[c], Nathalie Kupka[a], Urs Alexander Peuker [b], Martin Rudolph[a*]

a. Helmholtz-Zentrum Dresden-Rossendorf, Helmholtz Institute Freiberg for Resource Technology, Freiberg 09599, Germany

b. Institute for Mechanical Process Engineering and Mineral Processing, TU Bergakademie Freiberg, Freiberg 09599, Germany

c. School of Chemical Engineering and Technology, China University of Mining & Technology, Xuzhou, Jiangsu 221116, China

*corresponding author: m.rudolph@hzdr.de

0. Abstract

The formation of surface micro-bubbles induced by air nucleation on graphite surfaces and the air diffusion process in oversaturated water play important roles in increasing the recovery of graphite and other valuable minerals in flotation. A microscope equipped with a cuvette, a laser diffraction particle size analyzer, and single bubble pick-up experiments were combined with micro-flotation experiments to clarify these effects. The diffusion-controlled growth process of surface micro-bubbles was observed with a microscope. It can be shown that higher degrees of dissolved air can improve the probability of surface microbubbles forming on graphite surfaces. Micro-flotation and microscopic experiments confirmed that surface microbubbles occurred selectively and only on graphite surface but not quartz. Besides, bubble-particle aggregates formed during the conditioning process were observed under the microscope while bubble pick-up experiments indicated that the bubble load increased with the increasing degree of dissolved air. Size distribution analysis also showed that the nucleation micro-bubbles on graphite surfaces improved the recovery of fine

graphite particles due to the formation of microbubble-particle aggregates . Coarser microbubble-particle aggregates induced by surface nucleation bubbles can improve the collision and attachment proability to external carrying bubbles as compared to single graphite particles, which is especially relevant for fine particles.

Keywords: surface micro-bubbles; air nucleation; diffiusion; flotation; bubble-particle flocs

1. Introduction

Surface nanobubbles or micro-bubbles on mineral surfaces in water caused by gas nucleation can enhance the attachment onto bubbles in flotation, sparking the interest of many scientists [1-4]. In flotation process, heterogeneous sites on mineral surfaces such as pores, crevices and valleys can provide gas nucleation sites along with pinning forces necessary for the stable formation of surface nano-bubbles and consequently micro-bubbles [5, 6]. Very sensitive towards pressure and temperature, air molecules in water often diffuse into these gasnucleation sites to form surface nanobubbles and micro-bubbles in air oversaturated water (where it can be assumed that in all circumstances of flotation there is air dissolved in water). As known from the literature that surface nanobubbles improve mineral flotation efficiency due to great advantages in several aspects: selective nucleation on hydrophobic mineral surfaces, enhancing the attachment to bubbles by gas capillary bridging, aggregates formation and reduction of flotation reagent consumption by acting as a secondary collector [1, 2, 7, 8].

Studies over the past two decades have shown that gas nuclei on the solid surface can reduce the nucleation energy barrier significantly [9, 10]. A considerable amount of literature has been published on the behavior of gas entrapment on solid surfaces. These studies suggest that the stability of these pre-existing surface gas plays an important role in the gas nucleation process. Their stability in water is influenced by the radius of curvature of the meniscus and gas saturation, which in turn depends on the wettability of the solid surface and the geometry of the nucleation site. Furthermore, the stability can be enhanced by the adsorption of surfactants in the gas-liquid interface [6]. In mineral flotation, the stability of gas nuclei on mineral surfaces can be improved by the

increase of hydrophobicity and the addition of surfactants. As a result of their increased stability, more surface nanobubbles/microbubbles will form. In addition to these factors, pressure also plays a significant role in the gas nucleation process [11], for example, a sudden pressure reduction will supersaturate the solution at the same time. In flotation devices, the high shear flow is utilized to mix pulp and disperse coarser bubbles to microbubbles. Meanwhile, this high shear can also induce significant pressure fluctuations, which in turn increase the gas nucleation probability on mineral surfaces.

Tao and Sobhy (2019) visualized the particle trajectory moving around the surface of a regular-sized flotation bubble and found that the time required for the rupture of the thin film between the particles and the bubble in the presence of surface nanobubbles induced by alcohol-water exchange was 50 % faster than that of particles without surface nanobubbles [12]. Ozun et al. (2019) found that cold water saturated with CO_2 promoted the flotation rate and flotation recovery of oxidized pyrite significantly and tiny bubbles on the pyrite surfaces were considered to be the reason for the increased recovery [13]. Zhou et al. (2020) found that, when surface nanobubbles induced by a rise in temperature and stably nucleate on hydrophobized mineral surfaces, there was a higher attraction between muscovite particles. As a result, the number of aggregates increased, which promoted the flotation recovery. They also found surface nanobubbles selectively nucleate on the hydrophobic mineral surfaces [14].

In many studies of surface nanobubbles, the degree of gas saturation in the water near the surfaces is improved through the temperature-rising method or the alcohol-water exchange approach [13, 14,15]. Promoting surface nanobubble generation in a real flotation process using alcohol-water exchange would not be suitable as the alcohol residues on the mineral surfaces may prevent flotation, by e.g. deteriorating the stability of the froth. Thus, so far only the liquid temperature-rising is a reasonable method to induce surface nanobubbles in mineral flotation technical process. Typically, some methods for producing surface nanobubbles can also induce surface micro-bubbles on mineral surfaces. However, little attention has been put on surface micro-bubbles even though they may have more significant influences on mineral flotation. In flotation plants, there are many mechanical

devices such as pumps, mixers, and rotor-stators in the flotation cells which can suck and pressure air into the water to improve the degree of air saturation in recycling waters. The extremely stable gas nuclei on hydrophobic and rough mineral surfaces can significantly reduce the energy barrier for gas nucleation. This means that surface micro-bubbles can form on mineral surfaces in a very low degree of gas saturation under the influence of hydrodynamic conditions.

Recently, the reuse of graphite from battery wastes has attracted considerable attention of many scientists [16]. However, the size of the graphite in the liberation products of these batteries is very fine, which causes many problems in graphite flotation. Fine particles are difficult to float due to the low probability of particle-bubble collision [17, 18]. To improve the recovery of fine particles, many methods such as adjusting flotation cell design to enhance the shear forces and increase turbulent energy dissipation or the use of macromolecule polymers for agglomeration flotation have been developed. The methods of inducing flocs or aggregates are often utilized to enlarge the particle size, which are normally sorted into three classes: selective flocculation, coagulation, and hydrophobic aggregation [19, 20]. The formation of agglomerates due to the additional attractive capillary forces induced by surface micro-bubbles and nanobubbles is considered to be a possible reason for the increased floatability of fine particles.

Dissolved air flotation (DAF) is a process relying on gas nucleation in saturated water to remove colloidal particle contaminants from wastewater. In DAF, microbubbles are generated by saturated water passing through a pressure reduction nozzle, and these microbubbles collide with suspended colloidal particles and form bubble-particle agglomerates. However, the purpose of DAF is to recover all solid contaminant particles regardless of their wettability and little is known about the selectivity of the microprocesses, e.g. gas nucleation. Gas saturated water usually is obtained by mixing air and water in an air saturator under high pressure (3-8 bar). The dissolved gas in the liquid is the source of the bubbles in DAF, which is too low for application in mineral processing because the volume of the gas bubbles produced in DAF is far lower than that in mechanical flotation cells [21-23]. In this context, the main objective is to investigate the influences of surface micro-bubbles induced by gas nucleation on graphite flotation. Nucleation mechanisms reported in this study

should also contribute to a better understanding of DFA processes on a microscopic scale.

2. Materials and methods

2.1. Materials

The graphite sample was purchased from ProGraphite GmbH, Germany with 99.99 % carbon content. The d_{50} of the graphite used in the experiments was 22 μm. Quartz sample as the representative hydrophilic gangue mineral was purchased from Krantz Mineralienkontor, Germany. The d_{50} of the quartz used in the experiments was 96 μm. The quartz sample was not ground to the same size range as graphite because particle size has little influence on the floatability of quartz in pure water without reagents and coarser quartz particles have relatively more heterogeneous spots to act as air nucleation sites. The quartz sample were washed in 6N HCl aqueous solution (Carl Roth GmbH, 37 %) for 10 min to remove possible contaminations. To investigate the effects of air nucleation on the (fine) graphite flotation, a pressure tank connected to a high-pressure air source was utilized for the preparation of water with different degrees of air saturation. Deionized water produced by our laboratory was sealed in the tank under 3 bar and 5 bar air pressure (overpressure) for 4 h (the produced waters are expressed as 3 bar and 5 bar water in the following part). The degree of air saturation increases with conditioning pressure according to Henry's law, i.e. the amount of dissolved gas in a liquid is proportional to its partial pressure above the liquid and the proportionality factor is Henry's constant.

2.2. Methods

2.2.1. Micro-flotation experiments

Graphite particles were dispersed in air saturated water in atmospheric conditions to generate surface microbubbles/nanobubbles, which were combined to coarser bubbles (the conventional bubbles in flotation) to improve flotation recovery. The micro-flotation experiments were carried out using a Hallimond tube at 19°C (±0.5°C) with 1 g pure graphite and a mixture of 0.8 g graphite

with 0.2 g quartz separately in the normal water and 5 bar water. The initial pH of the flotation solution was 7. No collector, frother, and other reagents was added in the micro-flotation experiments. 180 ml of flotation pulp (5.56 g/L) was agitated in a beaker using a magnetic stirrer for 2 min and then transferred to the Hallimond tube designed by TU Bergakademie Freiberg with air sparging through a frit. The Hallimond tube was equipped with a magnetic stirrer rotating at 500 rpm to disperse the particles, and the feed sample was further conditioned for 8 min within the Hallimond tube. After conditioning, the airflow was set to 20 cm^3/min for collecting concentrates and the total flotation time was kept as 4 min. After the flotation, the concentrates and tailings were filtered using a vacuum filter and dried at 50°C - 60°C in a drying oven until mass constancy was reached. The resulting mass balance was checked for losses and tests with losses above 10 % were rejected. The recoveries of the tailings and concentrates were calculated based on the tailing and concentrate masses. The carbon grade of the concentrates and tailings in the mixture flotation experiments was obtained by the combustion-loss method at 1000°C. At least three experiments were repeated for each data point.

2.2.2. Single bubble pick-up experiments

An optical contour analysis instrument (OCA50, DataPhysics Instruments GmbH, Germany) was used for the single bubble pick-up experiments investigate the variation of floatability of graphite particles in water with different degrees of air saturation. [24-26]. The experiments were performed at 19°C (±0.5°C). The procedure is shown in Fig. 1. First, a 2 g graphite sample was conditioning in an 80 mL closed cuvette in the waters with different degrees of air saturation using a magnetic stirrer at 1400 rpm for 8 min, and the magnetic stirrer was taken out immediately after agitation. After most of the particles settled to the bottom of the cuvette and the supernatant started clarifying, the cuvette was placed on the table of the OCA device, and a 100 μL air bubble was generated in the solution by a needle with 1.37 mm inner diameter connected to a glass syringe. The variations in bubble diameters are smaller than 5 %. The generated bubble was moved down slowly to get into contact with the graphite particle bed and was left in contact for 10 s. For each experiment, the lower end of the needle is set to the same horizontal position to keep the bubble-particle bed pressing and

bubble deformation constant. Then, the bubble was moved upwards for imaging and the tests were repeated 20 times at different positions for each condition.

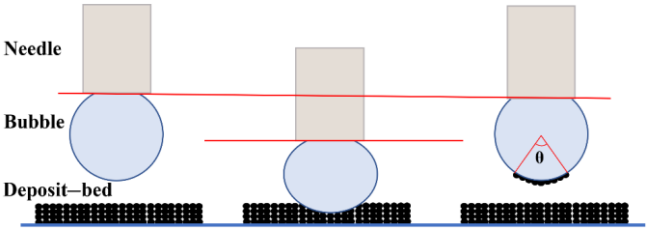

Fig. 1. Sketch of single bubble pick-up experiments

2.2.3. Agglomeration experiments with laser diffraction

Laser diffraction was utilized to investigate the (fine) graphite particle agglomeration performance in the air saturated waters. The size distribution of graphite (partially agglomerated) in the solution was analyzed with a laser diffraction device equipped with a cuvette (HELOS, Sympatec GmbH, Germany). The experiments were conducted at about 19°C (±0.5°C). The graphite particles were dispersed by a magnetic stirrer at 2500 rpm within the cuvette. A 30 mg sample was dispersed in 30 ml water conditioned at atmospheric pressure and 5 bar overpressure. After adding the particles, their size distribution after 60 s, 120 s, and 180 s were measured and compared. To avoid bubbles and flocs attaching on the cuvette wall and also the nucleation of air, the cuvette was cleaned and treated with oxygen gas plasma for 1 min before each experiment. The schematic diagram of the device is shown in Fig. 2. The measuring range of the optical lens in the tests is 0-875 μm.

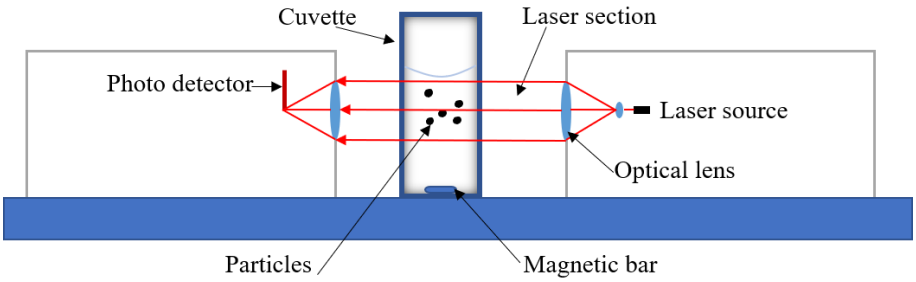

Fig. 2. Sketch of the laser diffraction device

2.2.4. Microscope experiments

A light optical microscope equipped with a special cuvette was used to observe the nucleation

process of surface microbubbles in the liquids at different degrees of air saturation. Before each experiment, the cuvette was cleaned with DI water, isopropanol (Carl Roth GmbH, ≥99.95 %), ultrasound, and processed in oxygen gas plasma for 1 min. The experiments were carried out at about 19°C (±0.5°C). The procedure of the experiments is as follows: first, about 20 mg particles were weighted for each experiment, and dispersed in a beaker with 40 mL liquid with a magnetic stirrer for 1 min. After the particles settled down to the bottom of the beaker, a pipette was used to transfer the deposited particles and liquid to the cuvette. The cuvette was then placed on the objective table for observation. 20 photos of different positions in the cuvette were taken for each experiment to view more surface micro-bubbles and to ensure the results are statistically representative. The samples were observed under 2.5 x, 10 x, and 20 x magnification.

3. Results

3.1. Micro-flotation and single bubble pick-up experiments

Fig. 3 illustrates the micro-flotation recovery of the pure graphite particles as a function of the conditioning overpressure of the liquid. As shown in Fig. 3, the average graphite recovery increased from about 50.4 % in normal water to about 62.8 % in 5 bar water. Fig. 4 shows the mass recovery and the carbon grade of the concentrates in the flotation experiments of the mixture samples with normal water and 5 bar overpressure conditioned water. The average mass recovery of concentrates increased from about 37.0 % in normal water to about 45.0 % in 5 bar water, and the carbon grades of concentrates in normal water and 5 bar water are about 98 %. The carbon grade of the concentrates is the same but the recovery is higher at higher overpressure. The separation efficiency (S_e) for the recovery of graphite from the mixture sample is given as:

$$S_e = \frac{R_c}{c_c} \times \frac{c_c - c_f}{100 - c_f} \times 100 \qquad (1)$$

R_c is the mass recovery of the concentrate (%), c_c is the graphite content of the concentrate (%), and c_f is graphite content of the feed (%). The separation efficiency increased from 42 % in normal water to 51 % in 5 bar water.

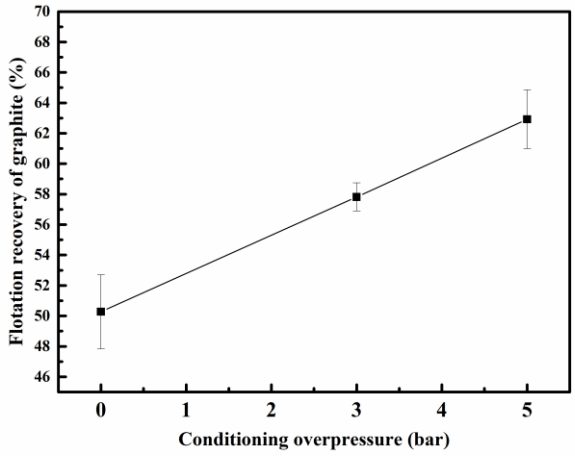

Fig. 3. The recovery of graphite against the overpressure in the pressure tank, the error bars represent the 95% confidence intervals

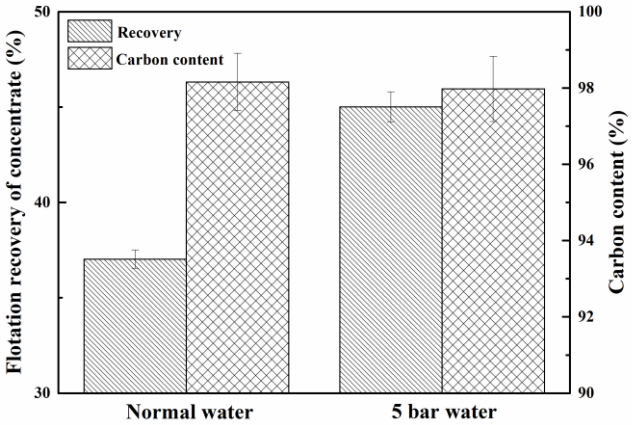

Fig. 4. The mass recoveries and carbon grades of the concentrates in the mixture of graphite and quartz flotation and the error bars represent the 95 % confidence intervals

Fig. 5 illustrates the average coverage angle of the pure graphite particles on the pick-up bubble surface as a function of the conditioning overpressure for the liquid in the single bubble pick-up experiments. The coverage angle can indicate the attachment probability of particles to bubbles as higher coverage angles mean more partciles attached onto the bubble. As shown in Fig. 5, the average coverage angle increased from 67.0° in normal water to 99.7° in 5 bar water, which means

more particles attached on the pick-up bubble in air oversaturation water and indicate the dissolved air can increase the attachment probability of graphite particles to bubbles in flotation. From the above experiments, it can be found that the dissolved air can selectively improve the floatability of graphite. It needs to be borne in mind that the contact time of particles and bubbles in micro-flotation is generally of the order of 10^{-2} s or less which is much smaller than the contact time for the pick-up tests which were at 10 s. This should be the reason for the stronger difference of floatability results but highlights the importance of air nucleation with respect to air saturation. The experiments did not allow to observe stronger particle agglomeration in the higher air saturation waters.

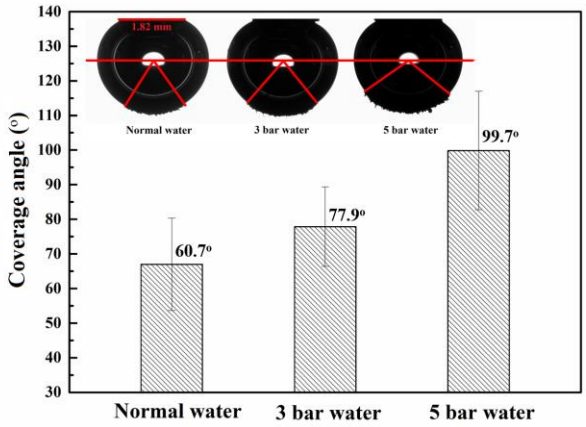

Fig. 5. The average cover angle of 20 single bubble pick-up experiments and the error bars represent the confidence intervals at $\alpha = 5$ %

3.2. Microscopic observations

It is difficult to observe bubble nucleation on ultra-fine particle surfaces. Hence, to investigate nucleation micro-bubbles in this study, a 20 μm sieve was used to separate the raw (pristine) graphite particles. The +20 μm fraction was used for microscopic observations. In order to properly observe the air nucleation on the graphite surfaces, a graphite substrate was immersed in the air saturated water. As shown in Fig.6, a surface microbubble in the red circle grew from a small nucleus in a rough spot on the graphite surface in 3 bar water under 20x magnification.

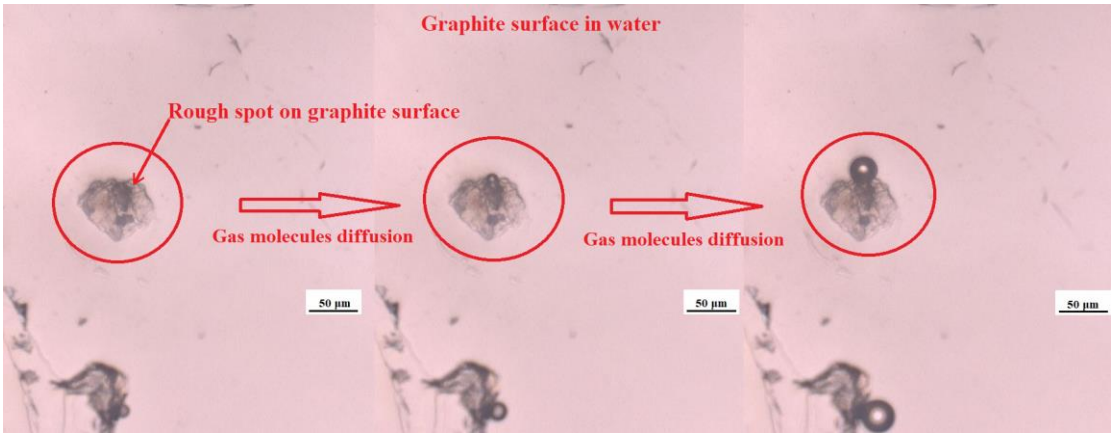

Fig. 6. The growth process of a nucleation bubble from a rough spot in 3 bar water under 20 x magnification

The growth process of surface microbubbles was recorded as shown in Fig. 7. The cuvette was moved underneath at 2.5x magnification to localize nucleation micro-bubbles on graphite surfaces. After several minutes, once the surface nucleation micro-bubbles grow to a size sufficient for visual detection, the magnification is changed to 10x to start recording the growth process of the single micro-bubbles. It is difficult to define the initial time of the nucleation process, so the first image is supposed to be obtained at approximately 0.5 min.

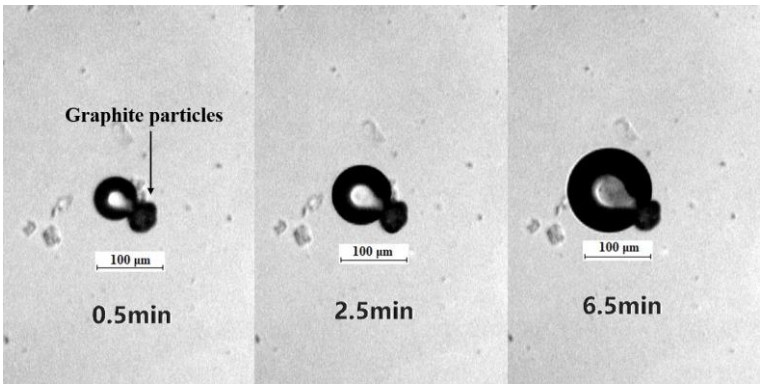

Fig. 7. The growth process of nucleation bubbles on the graphite particles in 3 bar water at 10x magnification

The growth rate of a diffusion-controlled spherical bubble in an infinite body of liquid (the effects of surface tension are neglected in the microscopic experiments of this study) has been calculated by Epstein and Plesset and the relationship of the bubble radius with time can be expressed by equation (2) [27-30]:

$$R = 2\beta\sqrt{Dt} \qquad (2)$$

where R is the bubble radius (μm), D is the mass diffusion coefficient (cm^2/s), t is the time (s), β is a dimensionless growth constant as expressed in equation (3)

$$\beta = \sqrt{\frac{c_s \xi}{2\rho_G}} \qquad (3),$$

where ξ is the degree of air saturation, c_s is the saturated air concentration at the liquid interface (mg/L), ρ_G is the density of air within the bubble (mg/L). The linear relationship between the diameter of a bubble and the square root of time also can be applied to the growth of a spherical cap bubble on a solid surface with the respective radius of curvature. In 3 bar and 5 bar waters, the diameters of the nucleation bubble on the graphite surface were nearly proportional to the square root of time as shown in Fig. 8, which indicates that air diffusion determines the growth process of surface micro-bubbles (the size differences of the bubbles in 5 bar water and 3 bar water are slight because a lot of micro-bubbles formed on the surfaces of graphite particles and the cuvette surfaces in 5 bar water, which changed the degree of air saturation ξ significantly).

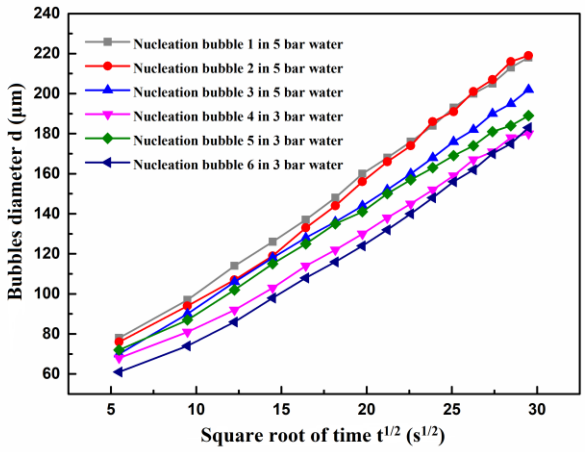

Fig. 8. The diameters of six representative micro-bubbles as a function of the square root of time in 3 bar water and 5 bar water

To estimate the formation probability of surface microbubbles, nearly 3000 particles were evaluated and the formation probability of surface microbubbles is defined as the ratio of the number of surface microbubbles n on the graphite particle surface to the number of graphite particles m. The probability of formation of surface microbubbles is defined as $p = (n/m*100\%)$. The micro-bubbles on graphite surfaces are marked by the circles in Fig. 9. The formation probabilities of surface microbubbles are 2.8 % in 3 bar water and 3.8 % in 5 bar water, which shows that the formation probability of surface microbubbles can be improved by the dissolved air, whereas in these

observations nothing can be said about the impact on surface nanobubble formation by the air saturation.

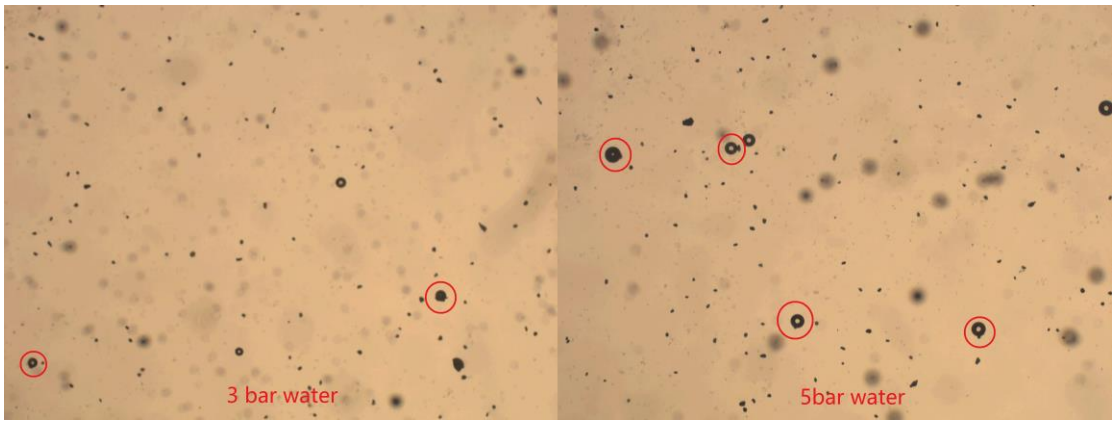

Fig. 9. Examplary micrographs of air nucleating bubbles on graphite surfaces for the statistics experiment of air nucleation probability in 3 bar water and 5 bar water, in total 18 such micrographs have been analyzed per pressure setting.

The mixture of graphite and quartz in 3 bar water was observed under the microscope. As shown in Fig. 10, the micro-bubbles only formed on the graphite surfaces, and no micro-bubbles were observed on quartz surfaces, which is consistent with the selectivity observed in the flotation experiments. During the conditioning process, after about 2 min agitation, a lot of flocs formed and floated to the top air-liquid interface and the flocs in 3 bar water were sucked into a pipette and transferred into the cuvette for observation under the microscope. As shown in Fig. 11, the flocs are composed of graphite particles and micro-bubbles, which are defined as aeroflocs.

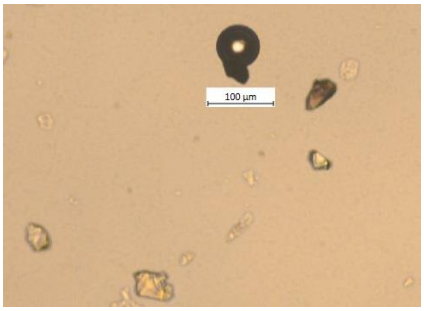

Fig. 10. Surface micro-bubbles on the graphite surface in the mixture of quartz (transparent) and graphite (black appearance)

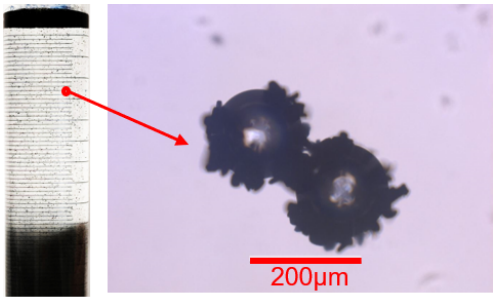

Fig. 11. The structure of an aerofloc in 3 bar water under the microscope

3.3. Agglomeration experiments

The size distributions of the feed (pristine) and the concentrates of the pure graphite flotation with normal water are shown in Fig. 12. The distribution of concentrates in normal water shifts to larger particle size compared to that of the pristine graphite. Most of the particles in the pristine graphite are very fine and the recovery of coarser particles is higher than fine particles in flotation.

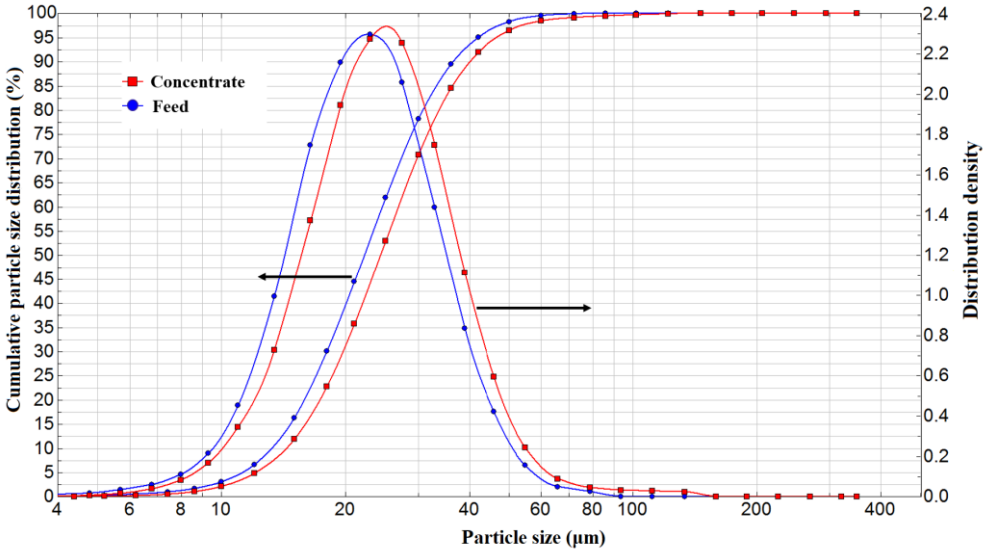

Fig. 12. The particle size distributions of the feed (pristine), and the concentrate of normal water flotation

To improve the formation probability and amounts of the aggregates, the +20 μm part of the pristine graphite was used for aeroflocs analysis with laser diffraction. Fig. 13 illustrates the size distribution of the +20 μm graphite in normal water and 5 bar water. As shown in Fig. 13, in normal water, the particle size distribution remains almost constant with time. On the contrary, in 5 bar water, the particle size distribution is varying with time. After 60 s agitation, some aggregates are formed, and the size of the aggregates is distributed in the range of 100 – 400 μm. After 120 s agitation, the

amount of aggregates declined due to the aggregates floating to the top liquid-air interface and moving out of the detection area. At 180 s agitation, the +80 μm size fraction in 5 bar doesnot show anymore as in the sample in the normal water. In Fig. 13, the red ellipse highlights these changes. The reasons for the preferential disappearance of coarse particles are suggested as follows: (i) surface micro-bubbles prefer to form on coarse particle surfaces due to more air nucleation sites such as crevices and rough spots, and (ii) the collision probability of coarse particles to micro-bubbles are higher than that of fine particles.

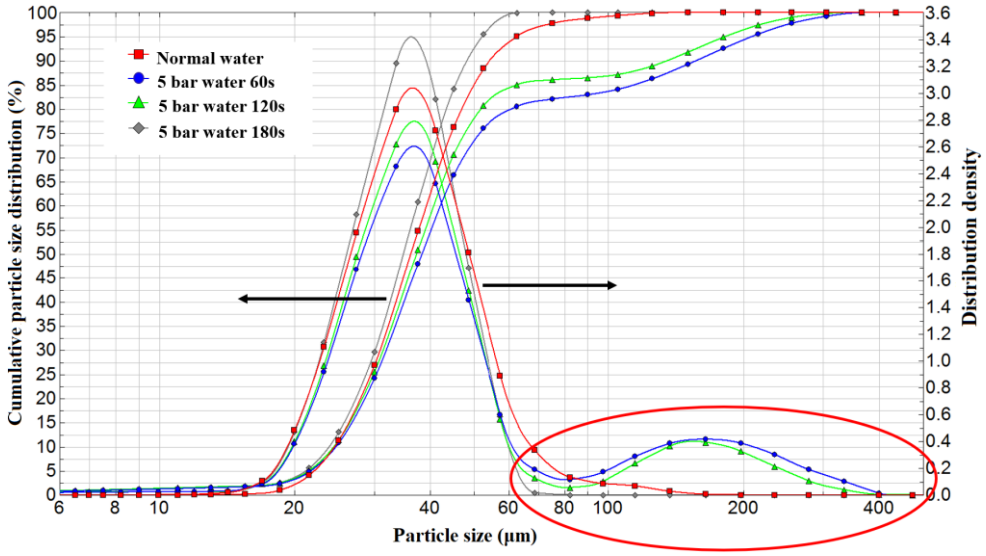

Fig. 13. The particle size distributions in normal water and 5 bar water after different times of measurement

4. Discussion

There are several reasons for a high flotation efficiency in air saturated water including (i) the generation of bulk microbubbles by air nucleating within the solution, (ii) the (selective) formation of surface nanobubbles and (iii) the (selective) micro-bubble nucleation on mineral surfaces. After releasing the pressure tank, some visible micro-bubbles can be generated in the water, which can also improve the flotation efficiency by attaching to the graphite particles. However, the density of the visible microbubbles is small in the water with a low degree of air saturation, and the collision and attachment probabilities will be low when the agitation speed of the magnetic rotor is rather slow. Besides, some of those microbubbles will float and disappear during the transfer process from the pressure tank to the flotation tube. As shown in Fig.7, no visible microbubbles on the surface of

the particles were found in 3 bar water at the beginning, and some visible microbubbles appear on the graphite surface after about 1 min, which means that the air nucleation bubbles on graphite surfaces play a more important role in 3 bar water. The bulk microbubbles also need to attach to the surface of minerals to become surface microbubbles to improve the flotation efficiency. After bulk microbubbles become surface microbubbles, these surface microbubbles will also grow due to the air diffusion and collision with other fine particles to form aeroflocs. As indicated in the introduction, many studies have displayed the importance of bulk microbubbles. Thus, the discussion in this study is mainly focused on air nucleation and air diffusion on the surface of the minerals.

From the microscope experiments, the air nucleation and air diffusion on mineral surfaces play important roles in flotation, especially in water with a low degree of air saturation. In the graphite flotation with air saturated water, dissolved air in water will diffuse into entrainment air nulei in the air nucleation sites such as crevices or heterogeneous pits. In a static condition, after several minutes, more air molecules diffuse into these air nulei to form surface nucleation micro-bubbles. Under the intense hydrodynamic conditions in real flotation scenarios, this process should be quicker than one minute. The smaller nucleation micro-bubbles on the mineral surfaces are assumed to improve the attachment efficiency of the fine particles with other fine particles, which leads to an improved collision efficiency of the resulting particle agglomerates with the carrying bubbles leading to an improved overall flotation recovery [20]. The degree of dissolved air improves the air nucleation probability on the graphite surfaces [31], and thus, the recovery of graphite. After the formation of surface micro-bubbles on the graphite surfaces, the micro-bubble carrying particles will collide with other graphite particles to form aeroflocs to further improve the recovery of fine graphite particles, which is the reason why with only 3.76 % formation probability of surface microbubbles in 5 bar water the overall recovery of graphite is already improved by nearly 12 %. The formation process of aggregates is schematically depicted in Fig. 14. The collision probability of large flocs to the coarser carrying bubbles is higher than that of a single fine particle. Additionally, and importantly, the air nucleation process is a selective phenomenon, and is more likely to appear on hydrophobic and coarse particles because of more air nucleation sites on these surfaces and a more stable bubble

contact. Based on the above description, surface micro-bubbles can act as a secondary collector in the flotation process to improve the recovery of graphite [32, 33].

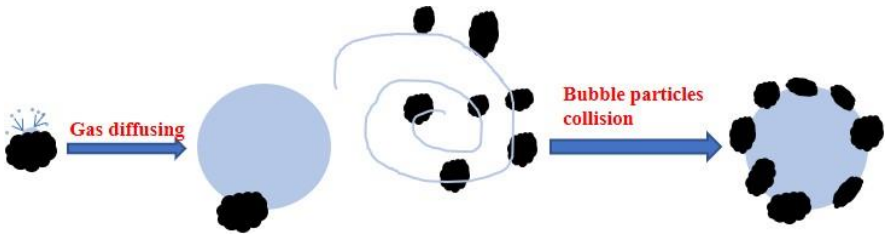

Fig. 14. Schematic representing the formation of surface micro-bubbles and formation of floating aggregates, the eddy is only pointing out turbulent conditions and must not necessarily be in scale as this is influenced by the different turbulent conditions.

Air nucleation is a universal phenomenon and plays an important role in flotation. However, there are still only a few studies for gas nucleation on mineral surfaces with varying hydrophobicity, hydrodynamic conditions, and surface morphologies. The degree of air saturation is not the only decisive parameter on the gas nucleation process. The surface characteristics such as wettability and roughness also have prominent influences on the air nucleation process, which as a consequence have a significant influence on flotation. As seen from the results forthe particle size analysis experiments, coarse particles are more likely to enter the flocs. It is assumed that coarse particle surfaces have relatively more heterogeneous surface spots to act as air nucleation sites which can increase the air nucleation probability on the surface of particles. More specifically, surface micro-bubbles can even form on some rough and hydrophobic surfaces such as coal and chalcopyrite in water with a very low degree of air saturation. Some flotation reagents such as collectors, promoters, and frothers can also influence the air nucleation probability and air diffusion process in the pulp. The hydrodynamic condition can enhance the mass diffusion process to accelerate the formation of surface micro-bubbles. Meanwhile, the pressure fluctuation on the mineral surfaces in the hydrodynamic conditions can also improve the air nucleation probability. In the investigation of fluid dynamics of flotation, air nucleation phenomena in air saturated water should be investigated more in depth, especially for some rough and hydrophobic minerals [34-37]. As mentioned before, some recycling waters in industry flotation are oversaturated with air. Different minerals have different surface roughness, wettability, size distribution, and reagent system. Thus, it is important

to investigate the influences of air nucleation on different flotation systems for a better understanding and possible optimization of the flotation process

5. Conclusion and outlook

In this study, the effects of surface micro-bubbles on the flotation performances of fine graphite particles were investigated by micro-flotation, single bubble pick-up experiments, microscopic observations, and agglomeration experiments. The flotation results showed that the flotation recovery of graphite increased with the degree of air saturation in water, and the flotation experiments with air saturated water showed good selectivity. The increase in the average coverage angles of graphite particles on bubbles in the pick-up experiments as a function of the degree of air saturation showed the promotion of the floatability of graphite particles, i.e. higher attachment efficiency on coarser carrying bubbles as well as higher collision efficiency induced by particle-bubble agglomerates e.g. aeroflocs. Microscopic observations indicated that the growth processes of nucleation micro-bubbles on graphite surfaces are controlled by air diffusion and the formation probability of surface microbubbles increases with the degree of air saturation. Besides, another important finding is that the surface micro-bubbles showed good selectivity and only formed on graphite surfaces in the mixture of graphite and quartz immersed in air saturated water. The aggregates, which are composed of micro-bubbles and graphite particles, were detected in the microscopic and agglomeration experiments during the agitation process, significantly improving the recovery of fine graphite particles by about 12 % even when the formation probability of surface microbubbles is only 3.76 % in 5 bar water. Moreover, coarse particles were seen to more easily enter aggregates and therefore the concentrates.

The wettability and roughness of minerals surfaces, hydrodynamic condition, ions and their species in solution, and reagent systems all have big influences on the air nucleation process in flotation. In the ongoing studies, the influences of these parameters on the air nucleation process and flotation performances are being investigated and will be reported in future papers. Furthermore, the results of this study can be applied in other mineral flotation systems and spark the investigation of other

parameters that can further influence the formation of surface nanobubbles, and micro-bubbles such as ions, surfactants, and especially the hydrodynamic conditions, i.e. pressure and pressure fluctuations.

Acknowledgment:
Ming Xu and Chenwei Li are funded by China Scholarship Council. The project is furthermore supported by fundings of the Helmholtz Foundation in PoF III (research program: Eneergy Efficiency, Materials and Resources). We would like to thank for the technical support by Klaus Graebe, Anja Oestreich and Edgar Schach, as well as the other colleagues of the processing department of the Helmholtz Institute Freiberg for helpful advice.

References:

[1] A. Azevedo, R. Etchepare, S. Calgaroto, J. Rubio, Aqueous dispersions of nanobubbles: Generation, properties and features, Miner. Eng. 94 (2016) 29-37.

[2] S. Calgaroto, K.Q. Wilberg, J. Rubio, On the nanobubbles interfacial properties and future applications in flotation, Miner. Eng. 60 (2014) 33-40.

[3] C.L. Owens, E. Schach, T. Heinig, M. Rudolph, G.R. Nash, Surface nanobubbles on the rare earth fluorcarbonate mineral synchysite, J. Colloid. Interface. Sci. 552 (2019) 66-71.

[4] C.L. Owens, E. Schach, M. Rudolph, G.R. Nash, Surface nanobubbles on the carbonate mineral dolomite, RSC Adv. 8(62) (2018) 35448-35452.

[5] M.A. Hampton, A.V. Nguyen, Accumulation of dissolved gases at hydrophobic surfaces in water and sodium chloride solutions: Implications for coal flotation, Miner. Eng. 22(9-10) (2009) 786-792.

[6] S.F. Jones, G.M. Evans, K.P. Galvin, Bubble nucleation from gas cavities-a review, Adv. Colloid Interface Sci. 80 (1999) 27-50.

[7] D. Lohse, X. Zhang, Surface nanobubbles and nanodroplets, Rev. Mod. Phys. 87(3) (2015) 981-1035.

[8] S. Nazari, S.Z. Shafaei, M. Gharabaghi, R. Ahmadi, B. Shahbazi, M.M. Fan, Effects of nanobubble and hydrodynamic parameters on coarse quartz flotation, Int. J. Min. Sci. Technol. 29(2) (2019) 289-295.

[9] D. Aquilano, E. Costa, A. Genovese, F.R. Massaro, M. Rubbo, Heterogeneous nucleation and growth of crystalline micro-bubbles around gas cavities formed in solution, Prog. Cryst. Growth Charact. 46 (2003) 59-84.

[10] H. Yuan, S. Tan, L. Feng, X. Liu, Heterogeneous bubble nucleation on heated surface from insoluble gas, Int. J. Heat Mass Transfer. 101 (2016) 1185-1192.

[11] N. Bremond, M. Arora, C.D. Ohl, D. Lohse, Controlled multibubble surface cavitation, Phys. Rev. Lett. 96(22) (2006) 224501.

[12] D.P. Tao, A. Sobhy, Nanobubble effects on hydrodynamic interactions between particles and bubbles, Powder Technol. 346 (2019) 385-395.

[13] S. Ozun, B. Vaziri Hassas, J.D. Miller, Collectorless flotation of oxidized pyrite, Colloids Surf., A. 561 (2019) 349-356.

[14] W. Zhou, C. Wu, H. Lv, B. Zhao, K. Liu, L. Ou, Nanobubbles heterogeneous nucleation induced by temperature rise and its influence on minerals flotation, Appl. Surf. Sci. 508 (2020) 145282.

[15] J. Fritzsche, U.A. Peuker, Particle adhesion on highly rough hydrophobic surfaces: The distribution of interaction mechanisms, Colloids Surf., A. 459 (2014) 166-171.

[16] J. Liu, H.Wang, T. Hu, X. Bai, S. Wang, W. Xie, J. Hao, Y. He, Recovery of $LiCoO_2$ and graphite from spent lithium-ion batteries by cryogenic grinding and froth flotation, Miner. Eng. 148 (2020) 106223.

[17] S. Farrokhpay, I. Filippova, L. Filippov, A. Picarra, N. Rulyov, D. Fornasiero, Flotation of fine particles in the presence of combined microbubbles and conventional bubbles, Miner. Eng. 155 (2020) 106439.

[18] B. Shahbazi, B. Rezai, S.M. Javad Koleini, Bubble–particle collision and attachment probability on fine particles flotation, Chem. Eng. Process. 49(6) (2010) 622-627.

[19] M. Krasowska, P.M.F. Sellapperumage, J. Ralston, D.A. Beattie, Influence of dissolved air on bubble attachment to highly oriented pyrolytic graphit, Physicochem. Probl. Miner. Process. 54(1) (2017) 163-173.

[20] T. Miettinen, J. Ralston, D. Fornasiero, The limits of fine particle flotation, Miner. Eng. 23(5) (2010) 420-437.

[21] V.R. Fanaie, M. Khiadani, Effect of salinity on air dissolution, size distribution of microbubbles, and hydrodynamics of a dissolved air flotation (DAF) system, Colloids Surf., A. 591 (2020) 124547.

[22] C. Karagüzel, Selective separation of fine albite from feldspathic slime containing colored minerals (Fe-Min) by batch scale dissolved air flotation (DAF), Miner. Eng. 23(1) (2010) 17-24.

[23] R.T. Rodrigues, J. Rubio, DFA-dissolved air flotation Potential applications in the mining and mineral and mineral processing industry, Int. J. Miner. Process. 82 (2007) 1-13.

[24] P. Chu, M. Mirnezami, J.A. Finch, Quantifying particle pick up at a pendant bubble: A study of non-hydrophobic particle–bubble interaction, Miner. Eng. 55 (2014) 162-164.

[25] E. Nowak, A.W. Pacek, Method for the prediction of the particle attachment to the bubble in oil at elevated temperatures, Powder Technol. 274 (2015) 105-111.

[26] D.I. Verrelli, B. Albijanic, A comparison of methods for measuring the induction time for bubble–particle attachment, Miner. Eng. 80 (2015) 8-13.

[27] P.S. Epstein, M.S. Plesset, On the stability of gas bubbles in liquid-gas solution, J. Chem. Phys. 18 (1950) 1505-1509.

[28] O.R. Enríquez, C. Sun, D. Lohse, A. Prosperetti, D. van der Meer, The quasi-static growth of CO_2 bubbles, J. Fluid Mech. 741 (2014).

[29] J. Li, H. Chen, W. Zhou, B. Wu, S.D. Stoyanov, E.G. Pelan, Growth of bubbles on a solid surface in response to a pressure reduction, Langmuir. 30(15) (2014) 4223-4228.

[30] Y. Wang, Z. Pan, F. Jiao, W. Qin, Understanding bubble growth process under decompression and its effects on the flotation phenomena, Miner. Eng. 145 (2020) 106066.

[31] L. Zargarzadeh, J.A.W. Elliott,. Bubble Formation in a Finite Cone: More Pieces to the Puzzle, Langmuir. 35(40) (2019) 13216-13232.

[32] P. Knüpfer, L. Ditscherlein, U.A. Peuker, Nanobubble enhanced agglomeration of hydrophobic powders, Colloids Surf., A. 530 (2017) 117-123.

[33] W. Zhou, H. Chen, L. Ou, Q. Shi, Aggregation of ultra-fine scheelite particles induced by hydrodynamic cavitation, Int. J. Miner. Process. 157 (2016) 236-240.

[34] E. Amini, D.J. Bradshaw, W. Xie,. Influence of flotation cell hydrodynamics on the flotation kinetics and scale up, Part 1: Hydrodynamic parameter measurements and ore property determination, Miner. Eng. 99 (2016) 40-51.

[35] E. Amini, D.J. Bradshaw, W. Xie, Influence of flotation cell hydrodynamics on the flotation kinetics and scale up, Part 2: Introducing turbulence parameters to improve predictions, Miner. Eng. 100 (2017) 31-39.

[36] H. Schubert, On the optimization of hydrodynamics in fine particle flotation, Miner. Eng. 21(12-14) (2008) 930-936.

[37] Z.A. Zhou, Z. Xu, J.A. Finch, J.H. Masliyah, R.S. Chow, On the role of cavitation in particle collection in flotation – A critical review, II, Miner. Eng. 22(5) (2009) 419-433.